2015 IEEE International Conference on Dependable Systems and Networks Workshops

Advantages in Crash Severity Prediction using Vehicle to Vehicle Communication

Dennis Böhmländer*§, Sinan Hasirlioglu*, Vitor Yano†‡, Christian Lauerer*, Thomas Brandmeier* and Alessandro Zimmer‡¶

*Institute for Applied Research, Ingolstadt University of Applied Sciences, Ingolstadt, Germany, 85049
Email: {dennis.boehmlaender, sinan.hasirlioglu, christian.lauerer, thomas.brandmeier}@thi.de
†Department of Communications, Electrical and Computer Engineering, University of Campinas, SP, Brazil, 13083-852
¶Institute of Technology for Development, Curitiba, PR, Brazil, 80215-090
‡Department of Electrical Engineering, Federal University of Paraná, Curitiba, PR, Brazil, 81531-970
Email: zimmer@eletrica.ufpr.br, zimmer@lactec.org.br, vitoryan@decom.fee.unicamp.br
§De Montfort University, Leicester, UK

***Abstract*—The paper discusses a new approach in contactless crash detection combining measurements of vehicle dynamics, exteroceptive sensors and vehicle-to-vehicle (V2V) communication data. The proposed architecture aims to activate vehicle safety functions prior an imminent collision to minimize the risk of suffering a major injury. An activation needs a precise prediction of time to collision (TTC), the crash severity (Cs) and other relevant crash parameters. This paper studies the contribution of V2V communication data to predict potential collisions and to realize a reliable activation. An algorithm is presented, that merges fused measurements of a video camera, a laser range finder (LRF) and ego vehicle motion sensors with V2V communication data to predict collisions. The benefit using V2V communication is demonstrated by evaluating collision prediction errors. This analysis is carried out based on experimental data produced by two scale model vehicles.**

I. Introduction

The World Health Organization (WHO) estimates traffic crashes to become the fifth leading cause of death by 2030 in the world. Especially low- and middle-income countries have a high road traffic death rate, for example Brazil with 22.5 traffic deaths per 100 000 population. Furthermore, the additional enlargement of motorization in these countries is expected to an increased number of traffic injuries and deaths within the next years [1]. Due to these developments, car manufacturers put very high priority to the development of new safety systems. Cooperative Intelligent Transport Systems (ITS) are attracting much attention to turn an elimination of fatalities into reality. Vehicle safety research focuses today on integrated safety systems to completely avoid accidents or, in case an accident does occur, to achieve an optimal and effective protection of the occupants and vulnerable road users (VRUs) (i.e. pedestrians). Integrated safety systems combine accident prevention and consequence mitigation.

In the near future, ITS will be able to communicate with each other and with traffic infrastructure in urban areas [2]. Main objectives of exchanging information between cooperative ITS are to improve vehicle safety and to enhance traffic or fuel efficient driving. Summer et al. [3] gives a detailed overview of inter-vehicle communication principles and technologies (e.g. WAVE (Wireless Access in Vehicular Environment) technology).

Most car crashes occur due to human failures, such as misjudgement of distance, driving operating errors or lack of attention [4]. It is evident that V2V communication can be used for precise warnings to the driver in critical and dangerous situations (e.g. traffic jam ahead or lane change warning) or for sending rescue messages after a severe traffic accident. Likewise, advanced applications, for example an active accident consequence mitigation is possible, using more details regarding the collision opponent.

A number of different studies show that triggering of new safety actuators shortly before a collision can significantly reduce the injury risk of the occupant. State-of-the-Art vehicles are equipped with three-point-automatic seat-belts in combination with air bag systems to reduce the passengers risk of injury. In comparison to standard occupant air bags, smart pre-crash systems can reduce loads in special cases up to 20% on average [5], [6]. External airbags and synthetic pressure hoses which are filled with gas prior to an impending collision can provide additional absorption [7]–[9].

First ideas to estimate optimal trigger times of an adaptive frontal restraint system for an oncoming collision using measurements of exteroceptive sensors can be found in [10], [11]. Westhofen et. al discusses in [12] a fusion of transponder position data and video camera data to trigger active safety systems with the focus on collision avoidance. Browne et al. presents in [13] an architecture to deploy occupant safety devices using fused measurement data of an exteroceptive sensor and a V2V communication. This approach includes an exchange of vehicle condition-defining signals in the case if the probability and the crash severity of a potential crash exceeds predefined thresholds. In this case the possible collision opponent is intended to provide information such as kinematic measurements (e.g speed, acceleration, yaw rate, etc.), geographic position data from a global navigation satellite system (GNSS) as well as crash relevant parameters (e.g mass, dimensions and stiffness).

This paper discusses an architecture to activate safety

978-1-4673-8044-7/15 $31.00 © 2015 IEEE
DOI 10.1109/DSN-W.2015.23

systems prior to an impending collision. The basic system idea is described in fig. 1. It consists of three main parts: perception, prediction and threat assessment. The proposed basic architecture is realized using two model vehicles to examine which kinematic and crash relevant measurements are needed to be communicated. For this purpose it is of particular interest, how the collision prediction accuracy can be improved regarding a fusion of exteroceptive sensor and V2V communication data. The described architecture does not take the geographic position data from GNSS into account since this data is in some cases imprecise or not available. The results are expected to contribute to a robust and secure realisation of future safety actuators triggered before an unavoidable collision.

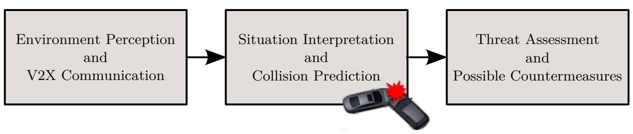

Fig. 1: Basic System Idea

Section II gives an overview of the intelligent crash prediction and necessary parameters. Two scale model vehicles are used to demonstrate and validate the proposed system in real crash scenarios. In section III the experimental design and the test results are presented. Finally, section IV presents the conclusions and future work.

II. Intelligent Crash Prediction Concept

The following part presents an intelligent crash prediction concept in detail describing a methodology to detect and track a potential collision vehicle as well as to predict the severity of an impending collision. The proposed concept is demonstrated in fig. 2. Measurements from a laser range finder (LRF), a video camera, and data from vehicle-to-vehicle (V2V) communication are fused in order to predict the time to collision (TTC) and the crash severity (Cs).

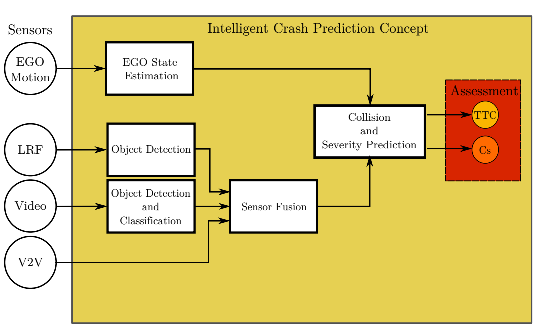

Fig. 2: Intelligent Crash Prediction Architecture

A. Collision Object Tracking

First of all the method to detect, classify and track the potential collision opponent is described.

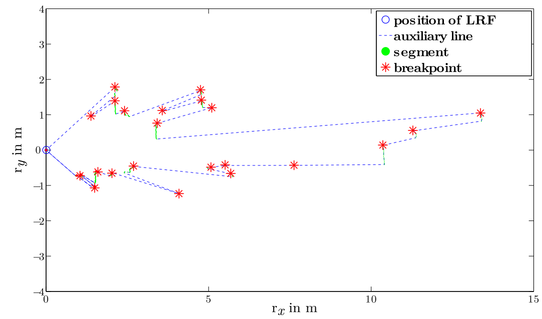

Fig. 3: Adaptive Breakpoint Detector and an Iterative End-Point Fit (IEPF) algorithm used to detect obstacles in the driving way

1) Collision Object Classification: In order to classify and detect nearby objects, measurements of a LRF and a video camera are used. In some cases the LRF data is not sufficient to generally determine to which class (e.g. car, bus, pedestrian, etc.) each object belongs to. On the other hand, data from the conventional monocular video camera does not carry depth information, what prevents an accurate computing of object positions and derived data [14], [15]. To take advantage of the information provided by both sensors, it is necessary to process them prior to the fusion. A decentralized approach is realized and the object detection is performed independently. The fusion is done afterwards in object level using selective measurements.

A combination of two state-of-art approaches, Integral Channel Features (ICF) [16] and Fast Feature Pyramids [17], serve for obstacle detection and classification in the video domain. The ICF approach extracts features from multiple channels of an image. Practical tests show that the image classification algorithm achieves 19% miss rate at 10^{-1} FPPI (false positive per image) for a rear and front car pictures Dataset.

The detection of objects from the LRF data is achieved by an Adaptive Breakpoint Detector and an Iterative End-Point Fit (IEPF) algorithm [18] (see fig.3). The first one is a method aiming to detect discontinuities (breakpoints) in the scanning surface that represent limits of the objects reached by the laser beam. In order to determine the breakpoints, Borges & Aldon propose an adaptive approach taking into account the noise associated for each distance measurement. The IEPF algorithm is used for line extraction afterwards, determining how many line segments are in the data, which points belong to which segment, and to estimate the model line parameters [19]. As the video object detection is much more complex than the LRF segmentation, the time gap between both steps can cause to an unsynchronization of the modules, which in turn is critical for a safety system operating in real-time. Hence the detector has to be applied only once per N frames. In every other frame, the objects positions are estimated based on the previous frame using the sparse optical flow method from Lucas-Kanade [20].

2) Sensor Fusion and Target Tracking: The fusion of the LRF and video camera measurements as well as the communicated V2V data are necessary to associate a class to the obstacles, discard false positive objects detected and to reduce the uncertainty of the measured relative positions and velocities of the objects. The target tracking is carried out with selective measurements after fusing all available information regarding the object.

In the first step, each valid object detected in the video camera image is associated to a set of line segments extracted from the LRF data. For this purpose, the line segments are projected onto the image space using the camera matrix of intrinsic parameters and corrected using the distortion coefficients of the lens. After that, for each of the detected objects, the relative intersection length of its bounding box and each set of line segments is computed. The set providing best results will be associated to this object. In order to avoid association of false positive detections, the detection is discarded in case the greater relative intersection is lower than 0.4. then, the sets of lines are associated to the received V2V data. The nearest neighbour method is used to associate the classified line segments to the corresponding communicated V2V vehicle data. The amount of data to be transmitted can vary depending on the application. The following data will be taken into account in this paper: velocity, mass, frontal stiffness and the geometrical dimensions of the collision partner. Theoretically, all messages on vehicle bus systems and all computed data of control units can be collected and transferred via V2V communication. Since this work investigates the V2V benefit in pre-crash, a rapid transmission of data is very important. A small amount of data contributes to the time of transmission. Furthermore, the change of the line position over time and the received velocity are compared in order to minimise the probability of false matches between ego vehicle's exteroceptive sensor and transmitted V2V data.

Once the data from all sources are fused on object level, selected kinematic measurements are fused for target tracking. Whenever the system receives a new sensor measurement the data fusion will be executed. A Cartesian coordinate system is chosen with its origin in the ego vehicle's centre of gravity (CG). The object position is relative to the ego vehicle. The object motion is estimated overground and rotated into the ego coordinate system [21], [22]. The ego vehicle is moving according to a continuous turn (CT) model with known turn rate [23] with its state vector $\mathbf{x}_n^{(EGO)} = \left[x_n \; v_{x,n} \; y_n \; v_{y,n} \; \dot{\psi}_n\right]^T$ at time step n, where x_n and y_n are the ego vehicle's CG position, $v_{x,n}$ and $v_{y,n}$ are the velocities in longitudinal and lateral direction and $\dot{\psi}_n$ is the yaw rate. The object's state vector at its CG can be written as: $\mathbf{x}_n = \left[r_{x,n} \; v_{x,n} \; a_{x,n} \; r_{y,n} \; v_{y,n} \; a_{y,n}\right]^T$, where $r_{x,n}$ and $r_{y,n}$ are the relative coordinates to the ego vehicle. $v_{x,n}$ and $a_{x,n}$ denote the object's velocity and acceleration over ground in longitudinal direction, $v_{y,n}$ and $a_{y,n}$ in lateral direction. The object motion model is given as:

$$\mathbf{x}_n = rot_n(\mathbf{F}_{CA}\mathbf{x}_{n-1} + \mathbf{u}_n + \mathbf{G}w_{n-1}), \tag{1}$$

where $\mathbf{F}_{CA}$ donates the state transition matrix based on a constant acceleration (CA) model [23], $\mathbf{u}_n$ the control vector, w_{n-1} the process noise sequence that is considered as a bivariate normal distribution with covariance matrix $\mathbf{G}$ and noise σ_x^2 and σ_y^2 along the two axis. Since the ego vehicle is performing a coordinated turn with angular velocity $\dot{\psi}_n^{(EGO)}$ during the sampling interval T the ego vehicle fixed coordinate system has to be updated using a rotation matrix:

$$\mathbf{rot}_n = \begin{bmatrix} \cos(\dot{\psi}_n^{(EGO)}T)\mathbf{I}_3 & \sin(\dot{\psi}_n^{(EGO)}T)\mathbf{I}_3 \\ -\sin(\dot{\psi}_n^{(EGO)}T)\mathbf{I}_3 & \cos(\dot{\psi}_n^{(EGO)}T)\mathbf{I}_3 \end{bmatrix}, \tag{2}$$

with $\mathbf{I}_3 = diag(1,1,1)$. The input vector is used to calculate the new object's relative position considering the ego vehicle's movement:

$$\mathbf{u}_n = \begin{bmatrix} -v_{x,n}^{(EGO)}\frac{\sin(\dot{\psi}_n^{(EGO)}T)}{\dot{\psi}_n^{(EGO)}} + v_{y,n}^{(EGO)}\frac{1-\cos(\dot{\psi}_n^{(EGO)}T)}{\dot{\psi}_n^{(EGO)}} \\ 0 \\ 0 \\ -v_{x,n}^{(EGO)}\frac{1-\cos(\dot{\psi}_n^{(EGO)}T)}{\dot{\psi}_n^{(EGO)}} - v_{y,n}^{(EGO)}\frac{\sin(\dot{\psi}_n^{(EGO)}T)}{\dot{\psi}_n^{(EGO)}} \\ 0 \\ 0 \end{bmatrix}. \tag{3}$$

The measurement model is given as:

$$\mathbf{z}_n = \mathbf{H}\mathbf{x}_n + v_n = \begin{bmatrix} 1\,0\,0\,0\,0\,0 \\ 0\,1\,0\,0\,0\,0 \\ 0\,0\,0\,1\,0\,0 \\ 0\,0\,0\,0\,1\,0 \end{bmatrix}\mathbf{x}_n + v_n. \tag{4}$$

Here, $\mathbf{H}$ is the observation matrix, v_n the measurement noise sequence with covariance matrix $\mathbf{R}$.

The target tracking uses fused LRF measurements and on-board motion data of the crash opponent vehicle transmitted by V2V communication. The LRF measurement vector in Cartesian coordinates is $\mathbf{z}_n^{LRF} = \left[r_{x,n}^{LRF} \; r_{y,n}^{LRF}\right]^T$ and object's motion measurement vector over ground transmitted via V2V communication is $\mathbf{z}_n^{V2V} = \left[v_{x,n}^{V2V} \; v_{y,n}^{V2V}\right]^T$. The fused measurement vector for target tracking can be written as:

$$\mathbf{z}_n^f = \left[r_{x,n}^{LRF} \; v_{x,n}^{V2V} \; r_{y,n}^{LRF} \; v_{y,n}^{V2V}\right]^T, \tag{5}$$

with the noise covariance matrix of measurement fusion:

$$\mathbf{R}^f = diag(\sigma^2_{r_{x,n}^{LRF}}, \sigma^2_{v_{x,n}^{V2V}}, \sigma^2_{r_{y,n}^{LRF}}, \sigma^2_{v_{y,n}^{V2V}}). \tag{6}$$

The motion and measurement model (eq. 1 and 4) are used in a discrete Kalman filter. For matrix $\mathbf{F}_{CA}$, matrix $\mathbf{G}$ and the implementation of the Kalman filter's state prediction and measurement update equations it is referred to [24].

B. Crash Severity Prediction

The estimated object state and the transmitted crash relevant information can be used to predict the probable collision. Based on the estimated object and ego state, it is possible to predict the time to collision (TTC) for a short-term. Different motion models can be used to predict the time of the collision. In [25] Lefvre et al. gives a detailed overview of interaction-aware, physics- and manoeuvre-based motion models. In the context of this paper it is assumed that the collision is unavoidable and the driver is no longer able to react. Thus, assuming constant relative velocity in the prediction interval, the TTC_n at the time step n can be calculated as follows:

$$TTC_n = \frac{\sqrt{(r_{x,n}^l)^2 + (r_{y,n}^l)^2}}{\sqrt{(v_{x,n}^{rel})^2 + (v_{y,n}^{rel})^2}}. \tag{7}$$

Beside the TTC, the severity of the impending collision plays a major role to correctly trigger occupant restraint systems. Vehicle collisions can be modelled and analysed using the fundamentals of engineering mechanics (principle of impulse and momentum). The crash pulse characteristics is an important variable to assess the occupants injury risk [26], [27]. Basic kinematic criteria associated with the crash pulse are today estimated during an accident (in-crash phase) to trigger occupant restraint systems. Basic criteria are, for example, the maximal acceleration a_{max}, the point in time when the vehicle velocity is zero $T_v = 0$, the change of velocity dV, and the OLC (Occupant Load Criterion). The OLC rates the occupant displacement and decelerations [28].

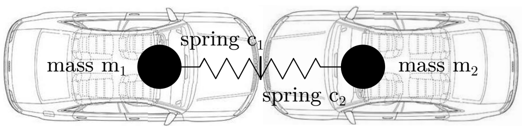

Fig. 4: Mass-spring-system for estimating crash pulse for a straight frontal vehicle-to-vehicle collision

The ego vehicle crash pulse can be modelled for a frontal collision by the following equations:

$$a_x^{(EGO)}(t) = \frac{\omega_1^2}{\omega}(V_{x,t_0}^{(Obj)} - V_{x,t_0}^{(EGO)})\sin(\omega t), \tag{8}$$

with:

$$\omega = \sqrt{\frac{c_{res}}{m_{res}}} = \sqrt{\frac{c^{(EGO)}c^{(Obj)}(m^{(EGO)} + m^{(Obj)})}{(c^{(EGO)} + c^{(Obj)})m^{(EGO)}m^{(Obj)}}}, \tag{9}$$

and

$$\omega_1 = \sqrt{\frac{c_{res}}{m^{(EGO)}}} = \sqrt{\frac{c^{(EGO)}c^{(Obj)}}{(c^{(EGO)} + c^{(Obj)})m^{(EGO)}}}. \tag{10}$$

The equation (8) is the solution of a mass-spring-system, where $m^{(EGO)}$ is the mass and $c^{(EGO)}$ the frontal mean-stiffness of the ego vehicle, $m^{(Obj)}$ the mass and $c^{(Obj)}$ the frontal mean-stiffness of the crash opponent. $V_{x,0}^{(Obj)}$ and $V_{x,0}^{(EGO)}$ are the velocities in x-direction of the ego vehicle and of the crash opponent at the time of the first contact $t_0 = 0$. Thus, the maximum ego-acceleration in x-direction $a_{x,max}^{(EGO)}$ can be calculated as follows:

$$a_{x,max}^{(EGO)} = |\frac{\omega_1^2}{\omega}(V_{x,t_0}^{(Obj)} - V_{x,t_0}^{(EGO)})|. \tag{11}$$

The frontal mean-stiffness $c^{(EGO)}$ and $c^{(Obj)}$ can be determined in various crash tests. Load cell moving barriers or load cell walls are used to measure force levels in frontal collisions [29], [30]. Together with the measured intrusion the frontal mean-stiffness can be derived for each vehicle type.

A comparative calculation helps to investigate the crash severity prediction error. Furthermore, the benefit of a precise knowledge of the opponents mean-stiffness and mass is analysed. Therefore, the frontal mean-stiffness of 30 vehicles is calculated using measured force levels in crash tests against a load cell wall [31]. The frontal mean-stiffness and mass are used to calculate $a_{x,max}^{(EGO)}$ and $OLC_x^{(EGO)}$ with equation 8. The error is calculated to the reference $a_{x,max,ref}^{(EGO)}$ and $OLC_{x,ref}^{(EGO)}$ with the statistical vehicle mean values of $m^{(Obj)} = 1800kg$ and $c^{(Obj)} = 450\frac{kN}{m}$. The results can be seen in fig. 5. The comparison result in an estimation mean error of 13% for $a_{x,max}^{(EGO)}$ and 13.4% for $OLC_x^{(EGO)}$. In comparison the $OLC_x^{(EGO)}$ error has higher outliers (up to 85%) than the calculated $a_{x,max}^{(EGO)}$ error.

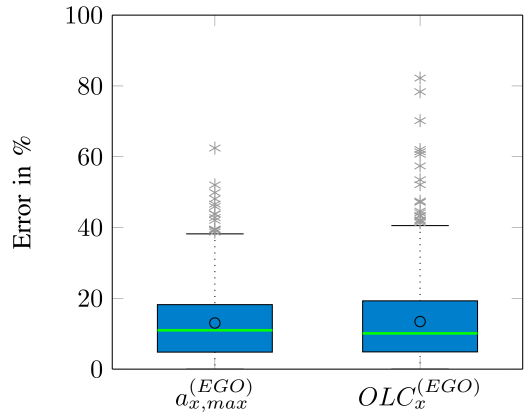

Fig. 5: Crash severity error analysis. Outliers are plotted as '*' and the mean as 'o'.

III. Test Method and Experimental Results

In the following section will be presented a test method to examine the collision estimation accuracy in real crash scenarios using two scale model vehicles. The resulting measurement data will be discussed.

A. Test Method

A scaled model vehicle, representing the ego vehicle, is used in two ways: as a trial bed for different pre-crash sensors and as an architecture to run the intelligent crash prediction concept presented in section II. EB Assist ADTF (Automotive Data and Time-Triggered Framework) is used to process the measured sensor data and to implement the concept in C++ programming language. The scale model is equipped with a Hokuyo UTM-30LX scanning LRF and a video camera (Microsoft LifeCam Studio with 75 degree horizontal FOV and 30 FPS) to detect objects nearby. The LRF is able to measure the object's horizontal contour and determine its position relative to the scale model in a range up to 30m. The LRF and the video camera are mounted on the scale model in an elevated position taking into special consideration their angles of view. A WLAN access point provides wireless connections to the on-board computers for remote control and to realize a V2V communication. Optical rev-counters are mounted and a Xsens miniature gyro-enhanced attitude (AHRS) is used to measure the vehicle's acceleration and velocity over ground. The scale vehicle is 1:5 model of a real vehicle and its dimensions can be summarized as follows: wheelbase 505mm, length 790mm and width 375mm.

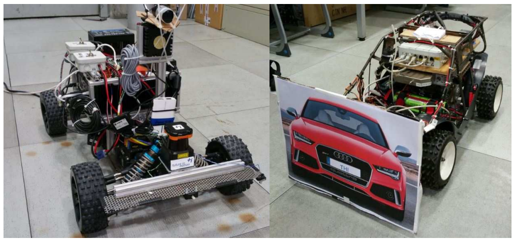

Fig. 6: Left: Scaled model vehicle (ego vehicle) with front bumper with contact switches. Right: The scaled target model with an exterior car picture on the front

A second model vehicle of the same scale is used as collision opponent. It is equipped with a sensor-architecture to determine it's self-movement precisely. Further the vehicle is able to transmit constant parameters and its measured movement (see eq. II-A2) with a frequency of $166Hz$ via WIFI using the User Datagram Protocol (UDP) transmission model. The scaled target model with an exterior car picture on the front can be seen on the right side in fig. 6. In order to guarantee the ability to classify the scaled target model, different car pictures must be bonded to the vehicles front or rear. Both scaled models are constructed to perform collisions, to capture the characteristics of a real collision and to benchmark the proposed algorithm experimentally (see fig. 6). For reasons of comparability, the collision velocities have been adapted. An overview of the relative collision velocities can be seen in table I. The corresponding closing velocities can be calculated using a conversion factor. This factor, here 0.2, has been defined by comparing geometric parameters (wheelbase, width, centre of gravity, etc.) between real vehicles and the scaled vehicle. To make the test reproducible the vehicles are accelerated with a lateral and longitudinal controller to the predefined collision velocity.

	Collision velocity in m/s	
	Reale Vehicle	Scaled Model Vehicle
Low speed test	4,4	0,89
Offset deformable barrier (40% overlap)	7,5 11,1 13,3 15,6	1,50 2,22 2,67 3,11
Full frontal (100% overlap)	11,1 15,6 17,8	2,22 3,11 3,56

TABLE I: Overview of frontal impact tests

B. Experimental Results

During this procedure various collisions with high overlap have been conducted with the two scaled model vehicles. These tests are intended to represent a real frontal crash scenario. Fig. 7 shows an example scenario using the sensor measurements (LRF, video camera, ego and motion sensors). In order to visualize an improvement using V2V data for pre-crash activation, the collision velocity and TTC is predicted. For each test, the TTC and collision velocity are predicted two times: One only with ego vehicles sensor measurements and the second one including the V2V communication data.

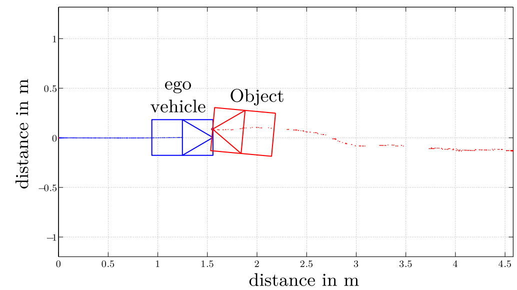

Fig. 7: Crash test scenario using two model vehicles, red dots mark the position measurements time history

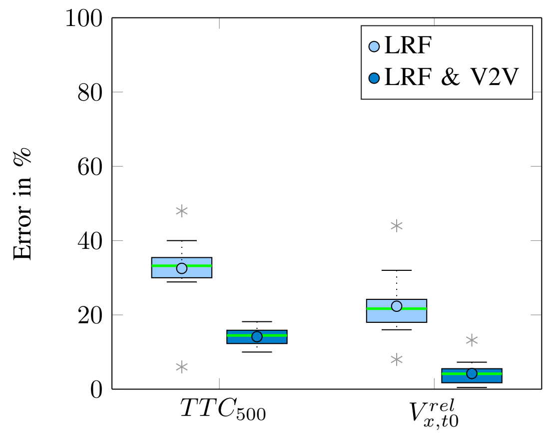

Fig. 8: Error comparison results from different test runs fusing LRF measurements and V2V data

After successfully realising a test collision, the TTC and relative velocity prediction at the moment $TTC_{500} = 500ms$ before collision is evaluated. In fig. 8 the evaluation can be seen. The collision velocity and the TTC prediction error are presented quantitatively using boxplots. It turns out, that the mean TTC error without V2V (33.6%) is higher than using V2V data (21.66%). Also the mean V_x error using V2V data is smaller (5%) compared to the mean error (14%) using ego sensors. This shows that the collision velocity and the TTC can be predicted more precise if communication data is available. The V2V communication can further provide object parameters such as height, length, mass and stiffness. For calculating a certain collision overlap, the received object width is an important value. The collision opponent width estimation based on the LRF measurements showed a 1.96% on average. This error can be compensated by V2V data. The Cs calculation can be improved with the transmitted mass and mean stiffness (see section II-B).

IV. Conclusion

In this paper, a concept of a contactless crash detection using fused measurements of various sensors is presented. A method to estimate a frontal vehicular collision using a video camera, LRF and a V2V communication to trigger safety functions earlier to reduce the occupant injury risk is described. The video classification for detecting pedestrians and vehicles is based on the ICF and the Fast Feature Pyramids method. The Adaptive Breakpoint Detector and the IEPF algorithm are used to determine the objects dimension and kinematics. The information is fused with V2V data of the potential collision vehicle afterwards. A Kalman filter is used to estimate the ego vehicle and object state with selective measurements. After that the collision severity and the TTC can be predicted for a short term. First results from impact tests using a scale model and a dummy or model vehicle showed a good behaviour. The results of the collision velocity and TTC prediction shows, that with an inclusion of V2V data the prediction quality increases. The TTC mean error using V2V data is 14.39% and the collision velocity mean error is 11.4% less than the reference mean prediction error without V2V data. A more accurate velocity estimation results from a more accurate TTC estimation. A further V2V communication advantage is that ego vehicle sensors blind spots can be compensated. The concept to predict vehicle-vehicle collisions presented in this paper has been demonstrated for frontal crashes with high overlap. To predict the severity in other crash scenarios, such as small overlaps and angular impacts, different crash models are needed. Finally, to transfer the knowledge to a full scale car the V2V communication standards have to be considered more in detail. Data rates, latency and communication range requirements for this safety application have to be studied and a trade-off has to be found.

ACKNOWLEDGMENT

The authors would like to thank the Coordination for the Improvement of Higher Education Personnel (CAPES), the Federal Ministry of Education and Research (BMBF), the German Academic Exchange Service (DAAD), Audi AG Ingolstadt and the Applied Network on Automotive Research and Education (AWARE) for the financial support and help.

REFERENCES

[1] World Health Organization (WHO), *Global status report on road safety 2013: supporting a decade of action*.

[2] Hannes Hartenstein and Kenneth P Laberteaux, "VANET: Vehicular Applications and Inter-Networking Technologies," *John Wiley and Sons*, 2010.

[3] C. Sommer and F. Dressler, *Vehicular Networking*. Cambridge University Press, Dec. 2014.

[4] Steven H. Bayless, Adrian Guan, Patrick Son, Sean Murphy, and Anthony J. Shaw, "Trends in roadway domain active sensing," in *Connected Vehicle Insights*. The Intelligent Transportation Society of America (ITS America), 2012.

[5] T. Wohllebe, M. Gonter, and M.-M. Meinecke, "Potential of pre-crash restraints in frontal collisions," Karlsruhe, Germany, Dec. 2006.

[6] G. Gstrein and W. Sinz, "Improvement of Airbag Performance through Pre-Triggering," *International Technical Conference on the Enhanced Safety of Vehicles*, 2009.

[7] S. Hakki and A.-H. Hakki, "Collision air bag and flotation system," U.S. Patent US20 080 309 060 A1, Dec., 2008.

[8] T. W. Chung, Y. S. Kim, S. H. Lee, and J. H. BAE, "Exterior airbag cushion for vehicle," U.S. Patent US8 764 062 B2, Jul., 2014.

[9] A. Loeffler and L. Quedenbaum, "Crashsicherheit eines Technologietraegers fr Elektrokleinstfahrzeuge," in *crash.tech*, Munich, 2014.

[10] R. Moritz, "Pre-crash sensing-functional evolution based on short range radar sensor platform," in *SAE Conference*, 2000.

[11] D. Wallner, A. Eichberger, and W. Hirschberg, "A novel control algorithm for integration of active and passive vehicle safety systems in frontal collisions," *Journal of Systemics, Cybernetics and Informatics*, vol. 8, 2009.

[12] D. Westhofen, C. Grundler, K. Doll, U. Brunsmann, and S. Zecha, "Transponder- and camera-based advanced driver assistance system," in *IEEE Intelligent Vehicles Symposium (IV)*, 2012.

[13] A. L. Browne, F. D. Wood, and O. D. Altan, "Pre-collision assessment of potential collision severity for road vehicles," U.S. Patent US8 321 092 B2, Nov., 2012.

[14] Z. Sun, G. Bebis, and R. Miller, "On-road vehicle detection using optical sensors: a review," in *The 7th International IEEE Conference on Intelligent Transportation Systems. Proceedings*, 2004.

[15] D. Geronimo, A. Lopez, A. Sappa, and T. Graf, "Survey of pedestrian detection for advanced driver assistance systems," vol. 32, no. 7, 2010.

[16] P. Dollár, Z. Tu, P. Perona, and S. Belongie, "Integral channel features," in *British Machine Vision Conference*, 2009.

[17] P. Dollár, R. Appel, S. Belongie, and P. Perona, "Fast feature pyramids for object detection," *Pattern Analysis and Machine Intelligence, IEEE Transactions on*, 2014.

[18] G. Borges and M.-J. Aldon, "Line extraction in 2d range images for mobile robotics," *Journal of Intelligent and Robotic Systems*, vol. 40, no. 3, 2004.

[19] V. Nguyen, S. Gchter, A. Martinelli, N. Tomatis, and R. Siegwart, "A comparison of line extraction algorithms using 2d range data for indoor mobile robotics," *Autonomous Robots*, vol. 23, no. 2, 2007.

[20] B. D. Lucas and T. Kanade, "An iterative image registration technique with an application to stereo vision," in *Proceedings of the 7th International Joint Conference on Artificial Intelligence*, vol. 2. San Francisco, CA, USA: Morgan Kaufmann Publishers Inc., 1981.

[21] Tobias Dirndorfer, Michael Botsch, and Alois Knoll, "Model-based analysis of sensor-noise in predictive passive safety algorithms," 2011.

[22] R. Altendorfer, "Observable dynamics and coordinate systems for automotive target tracking," in *2009 IEEE Intelligent Vehicles Symposium*, Jun. 2009, pp. 741–746.

[23] X. Rong Li and V. Jilkov, "Survey of maneuvering target tracking. part i. dynamic models," *IEEE Transactions on Aerospace and Electronic Systems*, vol. 39, no. 4, Oct. 2003.

[24] Jitendra R. Raol, *Multi-Sensor Data Fusion with MATLAB*. CRC Press, 2009. [Online]. Available: http://www.crcpress.com/product/isbn/9781439800034

[25] S. Lefvre, D. Vasquez, and C. Laugier, "A survey on motion prediction and risk assessment for intelligent vehicles," *Robomech Journal*, vol. 1, no. 1, 2014.

[26] Matthew Huang, *Vehicle Crash Mechanics*. Dearborn, Michigan, USA: Crc Press Inc, 2002.

[27] Michael S. Varat, "Crash pulse modeling for vehicle safety research."

[28] L. Kuebler, S. Gargallo, and K. Elsaesser, "Characterization and evaluation of frontal crash pulses with respect to occupant safety," in *9th International Symposium and Exhibition on Sophisticated Car Occupant Safety Systems*, 2008.

[29] S. Takizawa, E. Higuchi, T. Iwabe, T. Kisai, and T. Suzuki, "Study of Load Cell MDB Crash Tests for Evaluation of Frontal Impact Compatibility," in *Proceedings of the 19th International Technical Conference on the Enhanced Safety of Vehicles, Washington DC*, 2005.

[30] M. B. Jerinsky and W. T. Hollowell, "NHTSAs review of high-resolution load cell walls role in designing for compatibility," 2003.

[31] NHTSA vehicle crash test database. [Online]. Available: http://www-nrd.nhtsa.dot.gov/database/veh/veh.htm